N94-23923

KALMAN FILTERING
APPLIED TO REAL-TIME MONITORING OF APOGEE MANEUVERS

Frédéric de BOER
MATRA MARCONI SPACE
Toulouse, France

Christian BARBIER
ALCATEL ESPACE
Toulouse, France

ABSTRACT

Part of the Space Mathematics Division in CNES, the Flight Dynamics Center provides attitude and orbit determinations and maneuvers during the Launch and Early Operation Phase (LEOP) of geostationary satellites.

Orbit determination is based on a Kalman filter method; when the 2 GHz CNES/NASA network is used, Doppler measurements are available and allow orbit determination during the apogee maneuvers. This method was used for TELE-X and TDF 2 LEOP (3-axis controlled satellites) and also for TELECOM 2 and HISPASAT (spun satellites): it enables us to follow the evolution of the maneuver and gives out a quite accurate estimation of the reached orbit.

In this paper, we briefly describe the dynamic models of the orbit evolution in both cases, "3-axis" and "inertial" thrust. Then, we present the results obtained for each case. Afterwards, we present some cases to show the robustness of the filter.

Key words: Kalman, real-time, apogee maneuvers.

1. REAL-TIME MONITORING PRINCIPLES

The principles of real-time orbit determination during apogee maneuvers have first been presented at 1985's CNES Congress by Bruno Belon and at 1992's IAF Congress by Didier Breton (Refs. 1-2).

The orbit determination is based on a Kalman filter method. The six orbital elements and the components of the thrust are estimated whenever a measurement is received. The measurements used are Doppler measurements.

The 2 GHz CNES-NASA network authorizes continuous Doppler measurements. The best results are obtained when the apogee maneuver occurs with TM/TC visibility of three different stations. In this case, the prime station provides 2-way measurements and composite measurements with the two other stations.

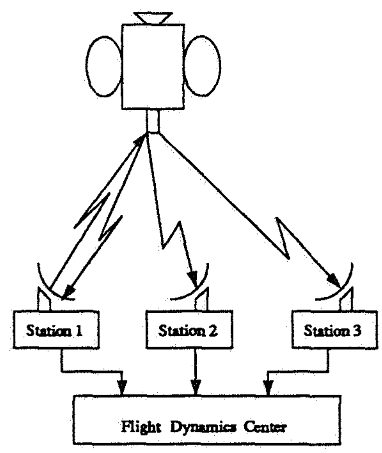

Three stations configuration

1.1 State Vector and Dynamics Model for a Three-axis Thrust

Kalman filtering is applied to the estimation of the following nine components state vector:

$l = v + w + \Omega$ $a = a$ $k = e \cos(w+\Omega)$ $h = e \sin(w+\Omega)$ $q = tg(i/2) \cos \Omega$ $p = tg(i/2) \sin \Omega$	equinoxial orbital parameters
γ_r γ_s γ_w	components of $\vec{F}/m$ ($\vec{F}$: thrust, m : mass) in the local orbital frame

Note : (a, e, i, w, Ω, v) are the keplerian parameters with v, the true anomaly.

The local orbital frame is defined as follows :

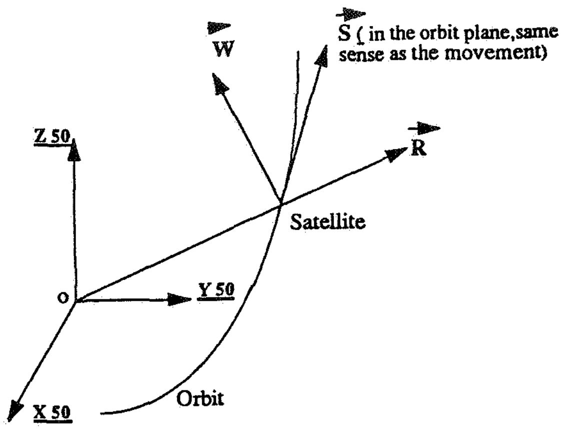

The three last components of the state vector are chosen to be adapted to "3-axis" satellites where the thrust has a fixed direction in the local orbital frame.

The evolution of the orbital elements is given by the Gauss equations :

$$\begin{bmatrix} \frac{dl}{dt}\\ \frac{da}{dt}\\ \frac{dk}{dt}\\ \frac{dh}{dt}\\ \frac{dq}{dt}\\ \frac{dp}{dt}\end{bmatrix} = \begin{bmatrix}G_{oo}\\0\\0\\0\\0\\0\end{bmatrix} + \begin{bmatrix}0&0&G_{13}\\G_{21}&G_{22}&0\\G_{31}&G_{32}&G_{33}\\G_{41}&G_{42}&G_{43}\\0&0&G_{53}\\0&0&G_{63}\end{bmatrix}\begin{bmatrix}R\\S\\W\end{bmatrix}$$

{G_{00}, G_{13}, G_{21}, G_{22}, G_{31}, G_{32}, G_{33}, G_{41}, G_{42}, G_{43}, G_{53}, G_{63}} are called gaussian coefficients. G_{00} corresponds to the keplerian movement.
R, S, W are the components of the perturbing acceleration in the local orbital frame (considered as an inertial frame).

And the evolution of the thrust acceleration is given by the three equations :

$$d\gamma_R/dt = q/m\ \gamma_R$$
$$d\gamma_S/dt = q/m\ \gamma_S \qquad q : \text{flowrate}$$
$$d\gamma_W/dt = q/m\ \gamma_W$$

This modelisation is only valid for a 3-axis thrust because it supposes that the components of the thrust are constant in the local orbital frame.

The nine-equation system of the dynamic model is integrated during the prediction phase of the Kalman filtering ; for this integration we need to compute R, S, W, the components of the perturbing acceleration due to the thrust (γ_R, γ_S, γ_W) and the acceleration caused by the J2 term of the terrestrial potential (every other perturbing factor is considered to be less important than the modeling error of the thrust).

1.2 State Vector and Dynamics Model for an "Inertial" Thrust

In the case of spun satellites during transfer (TELECOM 2, HISPASAT), the thrust has a fixed direction in an inertial frame. The dynamic model used for 3-axis transfer satellites, which supposed a fixed thrust direction in the local orbital frame, has to be adapted.

The state vector becomes :

l a k h q p	equinoxial parameters
γ_x γ_y γ_z	components of acceleration due to the thrust in $\Gamma 50$ inertial frame : F/m

With this choice, the dynamic model has a similar formulation to the 3-axis case.

$$\begin{bmatrix} \frac{dl}{dt}\\ \frac{da}{dt}\\ \frac{dk}{dt}\\ \frac{dh}{dt}\\ \frac{dq}{dt}\\ \frac{dp}{dt}\end{bmatrix} = \begin{bmatrix}G_{00}\\0\\0\\0\\0\\0\end{bmatrix} + \begin{bmatrix}G'_{11}&G'_{12}&G'_{13}\\G'_{21}&G'_{22}&G'_{23}\\G'_{31}&G'_{32}&G'_{33}\\G'_{41}&G'_{42}&G'_{43}\\G'_{51}&G'_{52}&G'_{53}\\G'_{61}&G'_{62}&G'_{63}\end{bmatrix}\begin{bmatrix}X\\Y\\Z\end{bmatrix}$$

$$d\gamma_X/dt = q/m\ \gamma_X$$
$$d\gamma_Y/dt = q/m\ \gamma_Y$$
$$d\gamma_Z/dt = q/m\ \gamma_Z$$

X, Y, Z are the components of the perturbating acceleration (thrust + J2 term of the terrestrial potential in Γ_{50} frame).

The new Gauss coefficients are obtained from the previous ones by the relation :

$$|G'_{ij}| = |G_{ij}| \cdot (R)$$

R is the rotation matrix from the local frame to the inertial frame Γ_{50}.

As for the "3-axis" satellites, the components of the perturbing force (X, Y, Z) take into account the components due to the thrust (γ_X, γ_Y, γ_Z) and the acceleration caused by the J2 term.

1.3 Measurement Model

When a frequency f_t is transmitted to the satellite and received back on the earth, the received frequency is fr = k f_t (1 - 2 V/c) (k is a satellite characteristic). The measurement of fr, which lasts a certain time Tc (counting time) provides V, the station-satellite removing velocity. In case of composite measurements (transmitting station different from receiving station), the measured velocity is the average of the removing velocities from the two stations.

In case of two-way Doppler measurements, the theoretical measurements V_{th} is given by :

$$TC.V_{th} = D(t + TC) - D(t)$$

D(t) is the satellite-station distance at the t date, D(t + TC) is the predicted satellite-station distance at t + TC. These two distances are computed as a function of the state vector. The measurements are taken into account in the correction phase of the filter.

2. APPLICATIONS

For practical applications during apogee maneuvers, the correction phase of the filter is only active from the beginning of the firing on. Before that, the orbit estimated by the software is only an extrapolation of the initial orbit (prediction phase of the filter). The measurements are used to correct the orbit only when the firing has begun. This appears clearly in the displays of the residuals shown in this paper immediately after the beginning of the firing, the correction makes the residuals decrease.

We will present now the results obtained in two cases :

- three-axis satellites,
- spun satellites.

2.1 Three-axis Satellite - TDF 2

The apogee maneuvers (first and third) during TDF2 LEOP occured with the visibility of three 2 GHz CNES stations : Kourou (KRU), Aussaguel (AUS) and Hartebeesthoeck (HBK).

On the graphic hereafter, the evolution of the semi-major axis and the residuals (after correction) during the firing are presented. Every time a new value of the semi-major axis is estimated, an estimation of the final semi-major axis is computed as a function of the current estimated orbit, the current estimated thrust and the remaining firing duration.

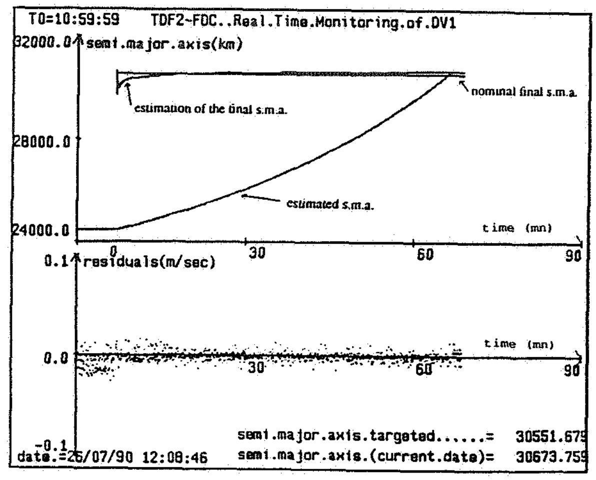

With regard to the first apogee maneuver, if we compare the real-time estimated orbit with the real orbit at the end of the firing, we notice that the results are very accurate. About one hundredth of degrees on w, Ω, M, one thousandth on i. For a, we reach a 5 km precision (to be compared with the difference between the real and the targeted orbit : 120 km).

The precision on the semi-major axis can be increased by following on the orbit restitution a few minutes after the end of the firing.

	Orbit at the beginning of the firing	Nominal orbit at the end of the firing	"Real" orbit at the end of the firing	Real-time estimated orbit at the end of the firing
Date	26/7/90 11h06'57.113"	26/7/90 12h06'41.114"	26/7/90 12h06'41.114"	26/7/90 12h06'41.114"
a (km)	24433.124	30551.677	30673.097	30668.092
e	0.7264	0.3820	0.3766	0.3768
i (deg.)	4.042	1.251	1.3747	1.3736
w (deg)	- 180.255	179.014	178.639	178.667
Ω (deg)	90.020	90.448	90.407	90.380
M (deg)	162.538	192.352	193.129	193.119

Nota : With regard to the third apogee maneuver, the precision on the semi-major axis obtained is around 10 km.

2.2 Spun Satellites : TELECOM 2, HISPASAT

2.2.1 TELECOM 2

Turning to TELECOM 2-A (first and third apogee maneuvers) and the first apogee maneuver of TELECOM 2-B, the firing occured with the visibility of KRU, AUS and HBK CNES stations.

Concerning the second apogee maneuver of TELECOM 2-B, the real time monitoring occured with the visibility of KRU, AUS CNES stations and Goldstone (GDS) NASA station. Hereafter, we present the results obtained for TELECOM 2-A first apogee maneuver, the other results are synthesized at the end of this chapter.

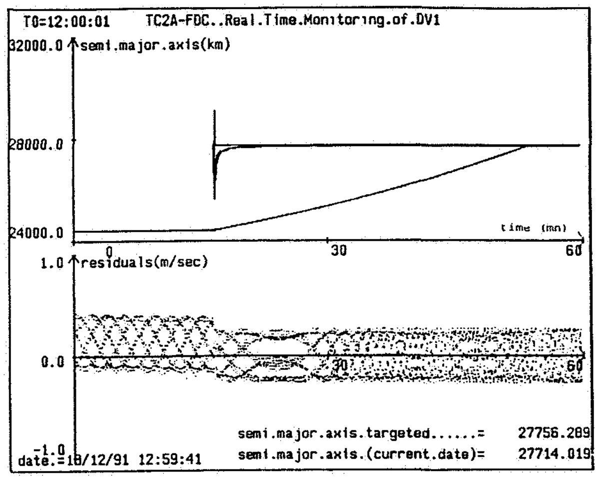

	Orbit at the beginning of the firing	Nominal orbit at the end of the firing	"Real" orbit at the end of the firing (computed 12 h later)	Real-time estimated orbit at the end of the firing
Date	18/12/91 12h16'36.864"	18/12/91 12h53'31.066"	18/12/91 12h53'31.066"	18/12/91 12h53'31.066"
a (km)	24415.89	27756.29	27719.67	27717.17
e	0.726	0.518	0.521	0.521
i (deg.)	3.983	1.914	1.959	1.9417
w (deg)	179.023	178.636	178.625	178.720
Ω (deg)	247.187	247.471	247.502	247.405
M (deg)	172.292	190.613	190.596	190.593

The precision on the estimated orbit is quite good (comparable with 3-axis satellites) though the fluctuations of the residuals are more important : 60 cm/s instead of 2 cm/s for 3-axis satellites.

The fluctuations of the residuals describe a periodic phenomenon which is caused by the rotation of the satellite. The Doppler measurements correspond to the velocity of S-band antenna with respect to the station. As the S-band antenna is not localized on the spin axis of the satellite, the measurement is the superposition of the periodic movement of the antenna with respect to the satellite gravity center and the movement of the satellite with respect to the station. The counting time lasts 2 seconds for CNES stations and the spin period is about 5 seconds. During some measurements, the velocity of the antenna will be added to the velocity of the satellite gravity center; during some others, it will be substracted.

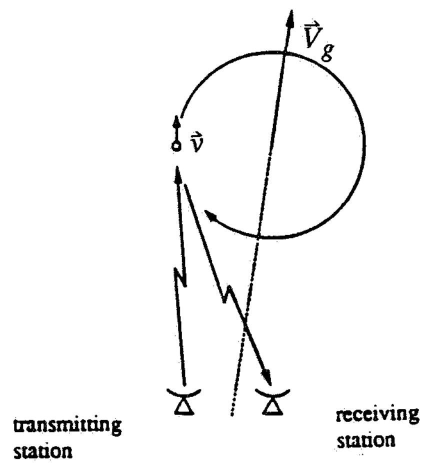

$\vec{V}_g$: satellite velocity in the station satellite direction,
$\vec{v}$: S-band antenna velocity with respect to the spin axis,

The received frequency is :

$$f_r = kf_e \cdot \left(1 - \frac{2}{c} \cdot \left(V_g + \frac{\vec{v} \cdot \vec{V}_g}{\|\vec{V}_g\|}\right)\right)$$

2.2.2 HISPASAT

The first and the third apogee maneuvers of HISPASAT occured with the visibility of HBK, AUS and KRU CNES stations. The precision obtained on semi-major axis is less than 5 km for the first maneuver.

	Orbit at the beginning of the firing	Nominal orbit at the end of the firing	"Real" orbit at the end of the firing	Real-time estimated orbit at the end of the firing
Date	12/09/92 11h54'21.914"	12/09/92 12h41'48.332"	12/09/92 12h41'48.332"	12/09/92 12h41'48.332"
a (km)	24347.74	29366.43	29284.81	29289.2
e	0.72954	0.43432	0.438334	0.438142
i (deg.)	6.966	2.643	2.725	2.673
w (deg)	178.989	178.305	178.192	177.919
Ω (deg)	151.431	150.306	150.461	150.739
M (deg)	173.332	197.819	197.829	197.824

The following figure shows the convergence of the estimation of the final semi-major axis during the maneuver. This convergence is reached about 10 minutes after the beginning of the firing and the deviation with respect to the "real" semi-major axis at the end of the maneuver is then less than 15 km.

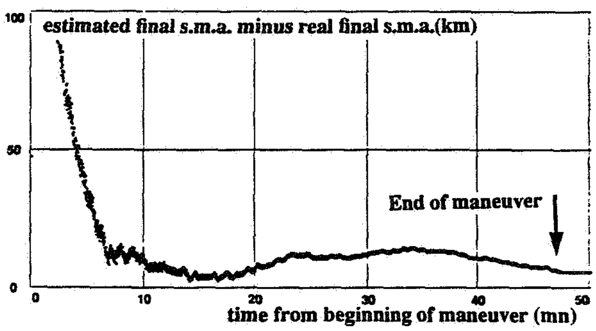

Estimated final semi-major axis minus "real" final semi-major axis during first maneuver

The third apogee maneuver monitoring gave a precision on semi-major axis of about 25 km just at the end of the maneuver. This relatively bad precision could be explained by the fact that the estimation of the final semi-major axis has not totally converged before the end of the firing. It is often the case for third apogee maneuvers which are usually very short. However, about ten minutes after the end of the maneuver, the semi-major axis has converged to less than 2 km of its "real" value.

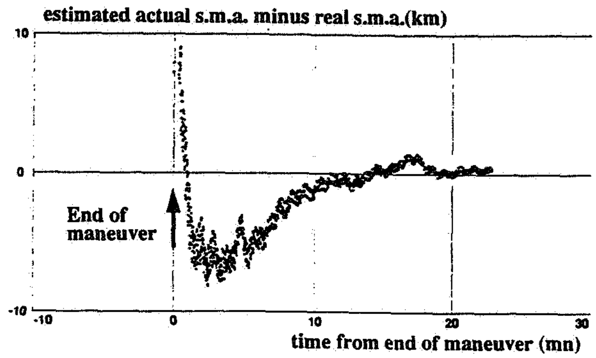

Estimated semi-major axis minus "real" semi-major axis after third firing

2.2.3 Synthesis of Results for Spun Satellites

Hereafter, we have summarized the results obtained in the case of TELECOM 2 and HISPASAT. We have compared the orbit computed a few hours after the maneuvers with the orbit estimated at the end of the firing.

The accuracy obtained for the semi-major axis is less than 10 km except for the second apogee maneuver of TELECOM 2-B. In that case, the elevation of the satellite seen from the station of Aussaguel was less than 5 degrees, the resulting bad quality of measurements could have contributed to this lack of precision. On the whole, the accuracy obtained on the other components of the orbit is quite good.

	Stations	Thrust duration	Da (km)	De	Di (deg)	Dw (deg)	DΩ (deg)	DM (deg)	DI (deg)
DV1 TC 2-A	KRU,AUS,HBK	2214.2	-1.79	$5\ 10^{-4}$	$-9\ 10^{-3}$	$8.3\ 10^{-2}$	$-8.6\ 10^{-2}$	$6\ 10^{-3}$	-
DV3 TC 2-A	KRU,AUS,HBK	227.4	6.04	$-8.1\ 10^{-5}$	$1.6\ 10^{-3}$	-	-	-	3.10^{-3}
DV1 TC 2-B	KRU,AUS,HBK	2270.8	-8.9	$4.87\ 10^{-4}$	$7\ 10^{-3}$	$7.1\ 10^{-2}$	$-6.6\ 10^{-2}$	-3.10^{-3}	
DV2 TC 2-B	KRU,AUS,GDS	3240.123	13.12	$-8.7\ 10^{-5}$	$-3.67\ 10^{-2}$	-	-	-	-0.1
DV1 HISP	HBK,KRU,AUS	2846.418	4.4	$-1.9\ 10^{-4}$	$-5.2\ 10^{-2}$	$-2.7\ 10^{-1}$	$2.8\ 10^{-1}$	-5.10^{-3}	-
DV3 HISP	HBK,KRU,AUS	278.218	< 1.	$3\ 10^{-5}$	$4.8\ 10^{-2}$	-	-	-	$9\ 10^{-3}$

Note : The values correspond to the orbit determined after a few minutes of convergence.

3. ROBUSTNESS OF REAL-TIME MONITORING

The software has shown a good behavior during all the apogee maneuvers and the orbital parameters obtained after the maneuvers were quite accurate. However, all these cases were nominal and no major problems were encountered. Furthermore, the only way to control the validity of the results is to compare them to an orbit determined after a few hours of ranging. A question that always arises at the end of the maneuver is : what confidence do we have in the orbit determined by the real-time monitoring ?

Some simulations have therefore been performed to test the robustness of the software to high dispersions on the thrust, on the attitude of the satellite, as well as delays on the thrust duration or on the maneuver beginning time. TC 2-A and HISPASAT first apogee maneuvers were considered and the simulation has consisted in monitoring these cases with wrong initial data. The considered cases were an underperformance of 50 N on the thrust (10 % of the nominal value), a bias of 5 deg. on the right ascension or on the declination of the thrust direction, and errors of 10 seconds on the thrust duration and the beginning time. It has to be noticed that these values are far above the specifications on these parameters, and can be considered as degraded cases.

The results obtained are quite good for all cases. The estimation of the final semi-major axis during the maneuver rapidly converges to the value obtained in the nominal case except for the error on thrust duration : the theoretical remaining duration is in that case different from the nominal one. The final orbital parameters at the end of the maneuver obtained after convergence are also quite accurate because the deviation with respect to the parameters obtained by the nominal real-time monitoring are of a few hundredths of degrees on w and Ω, a few thousandths on the mean anomaly.

The worst result obtained on the inclination deviation is of 1.5 hundredth of degrees obtained for the bias on the attitude. The deviation on the semi-major axis is always less than 2 km. The results for HISPASAT are gathered in table 3.1.

4. CONCLUSION

Real-time monitoring is possible when continuous Doppler measurements from three different stations are available. It enables us to follow the progress of the orbital parameters during the maneuver for three-axis stabilized satellites as well as for spun stabilized satellites. It provides then a quite accurate first diagnosis of the orbit a few minutes after the maneuver. The precision reached on the final orbit is of a few kilometers on semi-major axis. Moreover, the software has shown its robustness with respect to degraded cases on thrust amplitude or direction, as well as errors on the thrust duration or beginning time.

Another point is the fact that, with this software, we are able, as soon as the firing is over, to compute the new predictions (station visibilities, eclipses, ...), another apogee maneuvers strategy if necessary. Before, we had to wait many hours or to compute it with the targeted orbit.

REFERENCES

1. Belon, Bruno. Real-time determination during apogee maneuvers, CNES Congress, 1985.

2. Breton, Didier. Kalman filtering applied to real-time monitoring of apogee maneuvers. 43rd Congress of the International Aeronautical Federation, Washington, August 28-September 5, 1992.

Case	Da (km)	De	Di (deg)	Dw (deg)	DΩ (deg)	DM (deg)
50 N underperformance of the thrust	- 0.8	$6\ 10^{-5}$	$2\ 10^{-3}$	$1\ 10^{-2}$	$-2\ 10^{-2}$	$1\ 10^{-3}$
5 degrees bias on the initial thrust declination in $\Gamma 50$ frame	-0.2	$1.2\ 10^{-5}$	$1.5\ 10^{-2}$	$2.5\ 10^{-1}$	$2.5\ 10^{-1}$	$< 1\ 10^{-3}$
5 degrees bias on the initial thrust right ascension in Γ_{50} frame	-1.8	$1.4\ 10^{-4}$	$3\ 10^{-3}$	$3\ 10^{-2}$	$-3\ 10^{-2}$	$-6\ 10^{-3}$
10 s delay on the beginning time	+1.3	$4.5\ 10^{-5}$	$1\ 10^{-3}$	$3\ 10^{-2}$	$5\ 10^{-2}$	$5\ 10^{-3}$
Burn out 10 s earlier	-1.3	$2\ 10^{-5}$	$3\ 10^{-3}$	$1.6\ 10^{-1}$	$1\ 10^{-2}$	$2\ 10^{-3}$

Table 3.1